Eleventh International Conference on CFD in the Minerals and Process Industries
CSIRO, Melbourne, Australia
7-9 December 2015

DISCRETE ELEMENT MODELING OF PARTICLE FLOW BEHAVIORS IN A GAS-SOLID BUBBLING FLUIDIZED BED USING DYNAMIC RESTITUTION COEFFICIENT

Guodong LIU*, Fan YU, Huilin LU, Shuai WANG, Liyan SUN, Yanan ZHANG

School of Energy Science and Engineering, Harbin Institute of Technology, Harbin, 150001, China
*Corresponding author, E-mail address: gdliu@hit.edu.cn

ABSTRACT

The Discrete Element Model (DEM) is a very promising modelling strategy for particle-fluid two-phase systems. In this study, a small two dimensional gas-solid bubbling fluidized bed was simulated using DEM. A dynamic restitution coefficient for particle collisions was employed to simulate the wet particle flow behaviours by taking the energy dissipation of colliding particles into account. The influences of restitution coefficient, superficial velocity on the distribution of particle velocity, solid fraction as well as granular temperature distribution were investigated. It was found that the dynamic restitution coefficient could be well capable of predicting the collision process of wet particles. The time-averaged velocity of particles at low superficial velocity differs considerably between "dry" and "wet" particles, however, the difference decays with the increase of superficial velocity when energy dissipation for wet particles plays a less important role. Predicted granular temperature also follows a similar trend.

NOMENCLATURE

p	pressure
m	mass
$\boldsymbol{u}$	velocity
$\boldsymbol{g}$	gravity
$\boldsymbol{F}$	force
I	moment of inertia
$\boldsymbol{T}$	torque
r	radius
C_{d0}	drag force coefficient for single particle
ρ	density
μ	dynamic viscosity
ε	volume fraction
$\boldsymbol{\tau}$	viscous stress tensor
β_{int}	momentum exchange coefficient
ω	angular velocity of particle
δ	film thickness

subscript

p	particle
f	fluid

INTRODUCTION

Gas-solid fluidized beds have been widely applied to petroleum, chemical and energy industries, which involve highly complex gas-solid two phase flows. In the gas-fluidized bed, the fluidization is aggregative, where the gas phase will aggregate when the particle passes by, forming bubbles in the bed. Fluidization of dry particles could be well predicted by the continuous fluid model. However, the existence of liquid film gives rise to the increase of dissipative energy of solids. The energy dissipation of solid particles can change the interacting mechanism among colliding particles, thus it has an influence on the fluidization behaviour of particles, such as agglomeration and channel flow. This phenomenon could hazard some industrial applications.

In present work, we have used the DEM-CFD method, combining with the collision model for particles imposed by the interstitial fluid. A 2D bubbling fluidized bed experimentally investigated by Holland et al. (2008) was simulated. We simulated the fluidization of dry and wet particles with different superficial gas phase velocities, and the effect of the wet particle fluidization characteristics was obtained by comparing the distribution of particle velocity, solid fraction as well as granular temperature.

MODEL DESCRIPTION

The Discrete Element Method (DEM) (Cundall and Strack, 1979) treats the gas phase as continuum and solid phase as dispersed particles. The motion of solid particles follows Newton's second law. This method can trace the position and velocity of each individual particle by solving its own mass and momentum conservation equations. The typical forces considered are gravity and contact forces due to particle collisions. The open source software of MFIX-DEM was used in the simulation.

Equation for continuum phase

The fluid is the continuous phase, which follows the mass and momentum equations of conservation.

Continuum equation

$$\frac{\partial(\rho_f \varepsilon_f)}{\partial t} + \nabla \cdot (\rho_f \varepsilon_f \boldsymbol{u_f}) = 0 \tag{1}$$

Momentum equation

$$\frac{\partial(\rho_f \varepsilon_f \boldsymbol{u_f})}{\partial t} + \nabla \cdot (\rho_f \varepsilon_f \boldsymbol{u_f u_f}) = -\varepsilon_f \nabla p - \varepsilon_f \nabla \cdot \boldsymbol{\tau}_f + \varepsilon_f \rho_f \boldsymbol{g} + \boldsymbol{F_{int}} \tag{2}$$

$$\boldsymbol{\tau_f} = \mu_f [\nabla \boldsymbol{u_f} + (\nabla \boldsymbol{u_f})^T] - \frac{2}{3} \mu_f (\nabla \cdot \boldsymbol{u_f}) \boldsymbol{I} \tag{3}$$

Equation for dispersed phase

Particles suspended in the fluid suffer complex forces, such as the drag force $\boldsymbol{F_d}$, gravity force $\boldsymbol{F_g}$, buoyant force $\boldsymbol{F_b}$, contact force $\boldsymbol{F_{ci}}$, pressure gradient force $\boldsymbol{F_p}$ etc. By neclecting the virtual mass force, *Basset* force, *Magnus* force, *Saffman* force etc, the motion equation for solid particles is

$$m_p \frac{d\boldsymbol{u_p}}{dt} = \sum \boldsymbol{F} = \boldsymbol{F_d} + \boldsymbol{F_g} + \boldsymbol{F_b} + \boldsymbol{F_{ci}} + \boldsymbol{F}_p \tag{4}$$

$$I_p \frac{d\boldsymbol{\omega_p}}{dt} = \boldsymbol{T_p} \tag{5}$$

Drag force

For particle phase, the drag force can be expressed as

$$\boldsymbol{F_d} = \frac{\pi r_p^2}{2} C_d \rho_f \left|\boldsymbol{u_f} - \boldsymbol{u_p}\right| (\boldsymbol{u_f} - \boldsymbol{u_p}) \tag{6}$$

Gravity and Buoyant force

When particles are suspended in a fluidized bed, they suffer gravity and buoyant force due to the density difference among particles and the suspending fluid.

$$\boldsymbol{F_g} = \frac{4}{3}\pi r_p^3 \rho_p \boldsymbol{g} \tag{7}$$

$$\boldsymbol{F_b} = -\frac{4}{3}\pi r_p^3 \rho_f \boldsymbol{g} \tag{8}$$

Contact force

Assuming that the two colliding particles have the same mean radius *r*, each is represented with subscript *i* and *j*. The stiffness coefficient for colliding is $\boldsymbol{\kappa}$, the damping coefficient is $\boldsymbol{\eta}$, the frictional coefficient is ξ, and the contact force of particle *j* on particle *i* is $\boldsymbol{F}_{ij}$. Similar to the method used by Darabi et al (2011), the normal and tangential projections are:

$$\boldsymbol{F_{nij}} = (-\kappa_n \delta_n - \eta_n \boldsymbol{G}\cdot\boldsymbol{n})\boldsymbol{n} \tag{9}$$

$$\boldsymbol{F_{tij}} = -\kappa_t \delta_t \boldsymbol{t} - \eta_t \boldsymbol{G_{ct}} \tag{10}$$

$$\boldsymbol{G} = \boldsymbol{v_i} - \boldsymbol{v_j} \tag{11}$$

$$\boldsymbol{G_{ct}} = \boldsymbol{G} - (\boldsymbol{G}\cdot\boldsymbol{n})\boldsymbol{n} + r(\boldsymbol{\omega_i} + \boldsymbol{\omega_j}) \times \boldsymbol{n} \tag{12}$$

Where $\boldsymbol{G}$ is a relative velocity vector of particle *i* to that of particle *j*. $\boldsymbol{G_{ct}}$ is the tangential relative velocity at the contact point, $\boldsymbol{n}$, $\boldsymbol{t}$ represent the unit vectors at normal and tangential directions.

For the "dry" particle, damping coefficient $\boldsymbol{\eta}$ is constant, however, the damping coefficient differs with the variation of Stokes number for "wet" particles due to energy dissipation. The energy dissipation effect will be considered later on for the "wet" particles.

If $\left|\boldsymbol{F_{tij}}\right| > \xi \left|\boldsymbol{F_{nij}}\right|$, particle *i* begins to slide, and its tangential force can be expressed as:

$$\boldsymbol{F_{tij}} = -\xi \left|\boldsymbol{F_{nij}}\right| \boldsymbol{t} \tag{13}$$

If particle *i* collides with multiple particles simultaneously, the total force and total torque acting on particle *i* are:

$$\boldsymbol{F_{ci}} = \sum_j (\boldsymbol{F_{nij}} + \boldsymbol{F_{tij}}) \tag{14}$$

$$\boldsymbol{T_{ci}} = \sum_j (r\boldsymbol{n} \times \boldsymbol{F_{tij}}) \tag{15}$$

Besides acting force from other particles, fluidizing particles also suffer gravity, buoyant force, drag force etc. thus the total force of particle *i* in the fluidizing flow can be expressed:

$$\boldsymbol{F}_i = \boldsymbol{F}_{ci} + (\sum \boldsymbol{F})_i \tag{16}$$

From Newton's second law,

$$\dot{\boldsymbol{v}}_i = \frac{\boldsymbol{F}_i}{m} \tag{17}$$

Then particle velocity, position and angular velocity of particle *i* after a fixed time step Δt can be written:

$$\boldsymbol{v}_i = \boldsymbol{v}_i^{(0)} + \frac{\boldsymbol{F}_i}{m}\Delta t \tag{18}$$

$$\boldsymbol{r}_i = \boldsymbol{r}_i^{(0)} + \boldsymbol{v}_i \Delta t \tag{19}$$

$$\boldsymbol{\omega}_i = \boldsymbol{\omega}_i^{(0)} + \frac{\boldsymbol{T}_i}{I}\Delta t \tag{20}$$

Where the superscript (0) stands for the parameters of the last time step.

The particle-wall collision can be treated as particle colliding with another particle that has an infinite radius and velocity equals to zero.

If the material's Young's Modulus *E* and Poisson Ratio *v* are known, the stiffness coefficient $\boldsymbol{\kappa}$ can be calculated form the *Hertzian* contact theory, and the damping coefficient can be calculated using stiffness coefficient.

Pressure gradient force

When particles are fluidizing in a field where the pressure gradient plays a comparatively significant role, particles will suffer a force due to the pressure gradient:

$$\boldsymbol{F_p} = -\frac{4}{3}\pi r_p^3 \nabla p \tag{21}$$

Where *p* is the pressure distribution on the surface of the particle due to pressure gradient.

Momentum exchange coefficient

From the Two Fluid Model (TFM), the interface force acting on the control volume for model A (Gidaspow, 1994) is:

$$\boldsymbol{F_{int}} = \frac{\beta_{int}}{\varepsilon_f}(\boldsymbol{u_f} - \boldsymbol{u_p}) \tag{22}$$

Gidaspow (1994) combined the correlation of Wen & Yu (1966) for the fluid volume fraction $\varepsilon_f \geqslant 0.8$ and Ergun equation for $\varepsilon_f < 0.8$. In this research, we adopted the calculation method of Gidaspow, to calculate the momentum exchange coefficient.

$$\beta_{int} = \begin{cases} 0.75\rho_f C_d \dfrac{(1-\varepsilon_f)\varepsilon_f^{-1.7}}{d_p}\left|\boldsymbol{u_f} - \boldsymbol{u_p}\right| & \varepsilon_f \geq 0.8 \\ 150\dfrac{(1-\varepsilon_f)^2}{\varepsilon_f d_p^2}\mu_f + 1.75\dfrac{(1-\varepsilon_f)\rho_f}{d_p}\left|\boldsymbol{u_f} - \boldsymbol{u_p}\right| & \varepsilon_f < 0.8 \end{cases} \tag{23}$$

where

$$C_d = \begin{cases} \dfrac{24}{Re}(1 + 0.15Re^{0.687}) & Re \leq 1000 \\ 0.44; & Re > 1000 \end{cases} \qquad Re = \rho_f \varepsilon_f d_p \left|u_f - u_p\right| / \mu_f \tag{24}$$

Energy dissipation

In the process of fluidizing wet particles, the interstitial fluid effect should be taken into account. From the micro point of view, the existence of interstitial fluid can increase the forces acting on colliding particles, such as lubrication force, liquid bridge force etc. Appearance of these forces will increase the energy dissipation for

colliding particles, which thus impact on the motion characteristics of particles (Joseph, 2004, Apostolou, 2008).

The restitution coefficient is defined as the ratio of relative velocities after and before collision. It reflects the energy dissipation extent during the collision process.

$$e = -U_r / U_i \tag{25}$$

The interstitial fluid will increase the energy dissipation and thus has an effect on the restitution coefficient. Gollwitzer et al. (2012) conducted a series of experiments to investigate the interstitial fluid effect on the variation of restitution coefficient by tracing freely falling particles bouncing on a wet surface. The dependence of the restitution coefficient on the impact velocity and various properties of the particle (such as diameter, density etc.) and liquid (density and viscosity) was presented. The velocities of particles before and after collision were recorded by high speed camera, thus the restitution coefficient could be achieved. Energy loss in the collision process could be divided into two parts: one was from the contact of solid particles; the other was caused by the interstitial fluid among colliding particles. By combining fitting experimental results and energy dissipation analysis, a semi empirical correlation was observed to predict the wet particle restitution coefficient.

$$e_{wet} = (e_{dry} - \frac{3}{2}\frac{\rho_l}{\rho_p}\frac{\delta}{d_p}\frac{1}{e_{dry}})(1-\frac{14}{St}) \tag{26}$$

Where e_{dry} was the restitution coefficient for dry particles, and we used e_{dry}=0.976 in this study, and the liquid film thickness of $\delta = 0.1 d_p$ was employed in this study.

In DEM, we obtained the relationship between damping coefficient and restitution coefficient through solving free vibrating motion equation of viscous damping.

$$\eta_{wet} = \frac{2\sqrt{\kappa m}\ln e_{wet}}{\sqrt{(\ln e_{wet})^2 + \pi^2}} \tag{27}$$

Methods

In this simulation, the gas-solid fluidized bed was simulated, the width of the bed was 0.044m, and the height of the bed was 0.12m (Figure 1), and the humidity was 10%. At the initial, particles were generated randomly in the fluidized bed, after free sedimentation, they packed to form the initial bed. The wall condition was no-slip, the outlet of the bed was pressure outlet at the top, and the bottom was velocity inlet for the gas. Gas phase flowed into the bed uniformly from the bottom. In the gas-solid fluidization system. The resolution and time step checks had been done to check the grids resolution and time step accuracy. The simulation was conducted for 20s to fully consider the liquid film effect and make the system reach its steady state. The last 10s data was selected to make the time average figures. Detailed information for the parameters in the simulation was listed in Table 1.

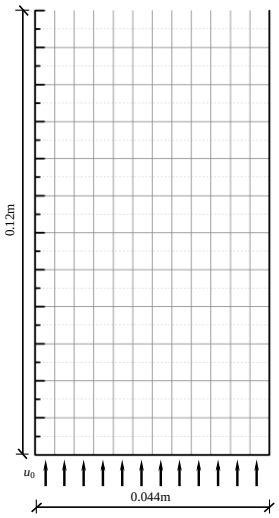

Figure 1: Schematic of the fluidized bed

Table 1: Parameters used in the simulation

Parameter	Value	Unit
Bed width	0.044	m
Bed height	0.12	m
Horizontal grids	12	—
Vertical grids	24	—
Particle diameter	0.5	mm
Particle density	900	kg/m^3
Number of particles	5000	—
Minimum fluidization velocity	0.13	m/s
Young's Modulus of particlest	1.2×10^5	GPa
Poisson ratio	0.33	—
Fluid density	1.2	kg/m^3
Fluid viscosity	1.8×10^{-5}	Pa • s

RESULTS

Effect of interstitial fluid on the distribution of particle velocity

For the dry particles, when the initial superficial velocity is two times of minimum fluidization velocity, time averaged axial velocity behaves symmetric distribution and radial velocity distributions follow a sin curve, however, for the wet particles, the velocity distributions are more flat at both directions. When the initial superficial velocity is three times of the minimum fluidization velocity of particles, difference between dry and wet particle velocity distributions become insignificant. It was the interstitial fluid which played an important role at the low velocity where liquid bridge force was significant, and particles would dissipate more energy to overcome the effect of liquid bridge, thus the velocity after collision decreased a lot.

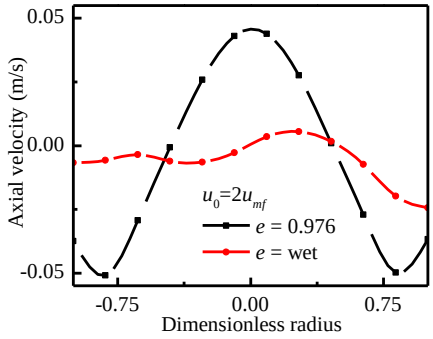

(a)

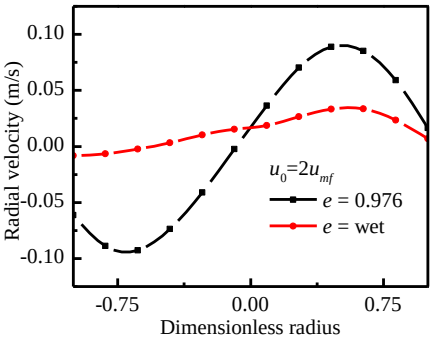

(b)

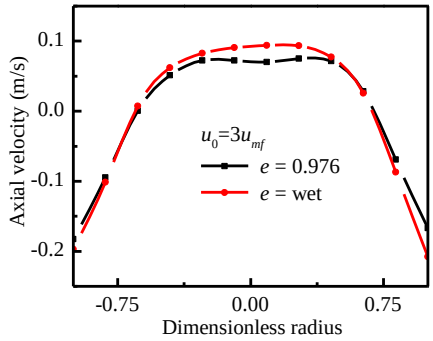

(c)

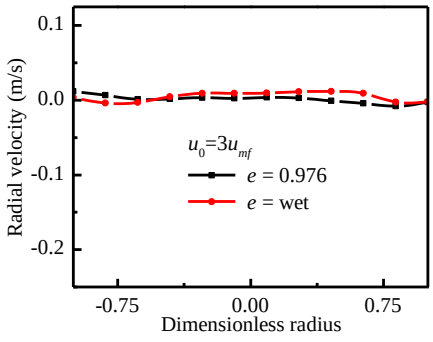

(d)

Figure 2: Particle velocity distributions at different initial gas phase velocity

Figure 3 shows the axial velocity fluctuation of particles. When the superficial gas velocity equals to $2u_{mf}$ (Figure 3 (a)), fluctuations of dry particles vary in a steady region, but fluctuations for wet particles have a higher amplitude. The differences between velocity fluctuations decrease with the increase of the initial superficial velocity (Figure 3 (b)).

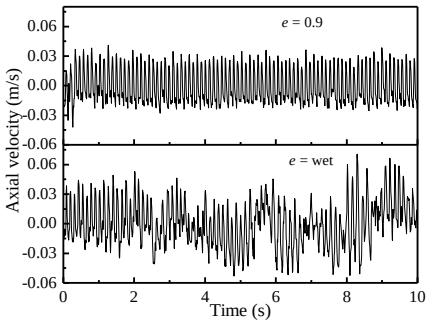

(a) $u_0 = 2u_{mf}$

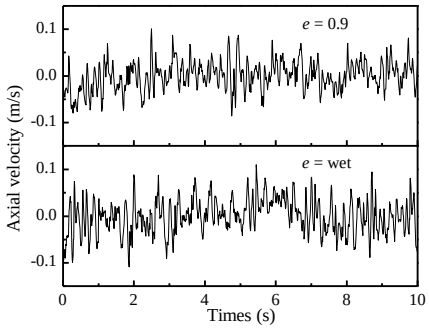

(b) $u_0 = 3u_{mf}$

Figure 3: Axial velocity fluctuations for particles at different initial conditions

Effect of interstitial fluid on the distribution of solid fraction

Figure 4 is the volume fraction distribution of particle phase. At lower superficial velocity, the interstitial fluid effect plays an important role. The difference between the centre and the walls of the bed is significant due to the effect of liquid bridge which consumes more energy during the process of particle collision. For higher initial velocity, volume fraction difference between wet and dry particles becomes obscure, because particles are easier to escape from the effect of liquid bridge due to their high stokes numbers.

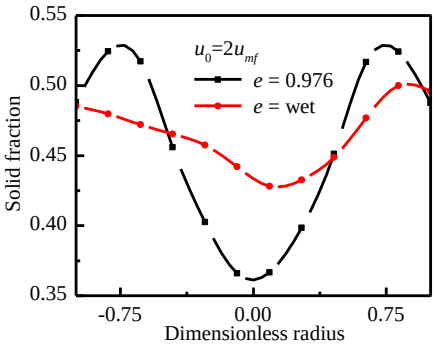

(a) $u_0 = 2u_{mf}$

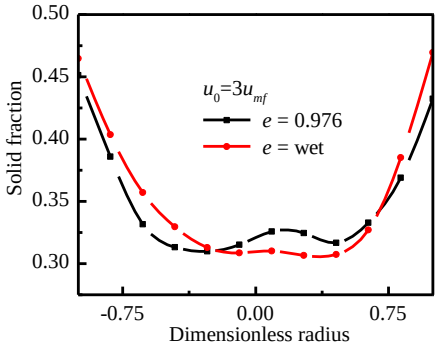

(b) $u_0 = 3u_{mf}$

Figure 4: Solid fraction distribution along the width of the bed

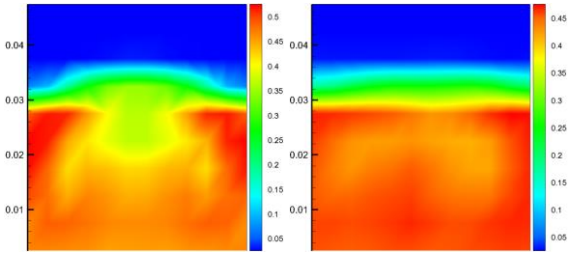

(a) $u_0 = 2u_{mf}$

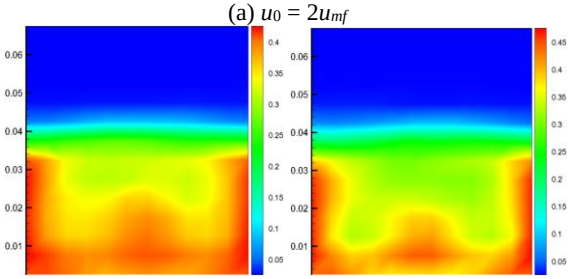

(b) $u_0 = 3u_{mf}$

Figure 5: Time averaged solid fraction distribution of dry (left) and wet (right) particles

Figure 5 shows the time averaged solid fraction distribution of dry and wet particles under different initial gas velocities. For the dry particles, when the initial velocity is $2u_{mf}$, obvious regions can be classified for particle concentrations. Existence of bubbles in the bed results in the low concentration region in the centre and high concentration region near the walls. However, at the wet condition, it is difficult to point out obvious bubbles, which is because the liquid bridge among colliding wet particles makes particles difficult to separate after collisions, when the gas phase passes by the bed, thus it is difficult for the gas phase to aggregate and form bubbles. When the initial gas phase velocity is $3u_{mf}$, bed height increases and formation of bubbles also changes. Since the liquid bridge effect is not as obvious as that for low stokes numbers, particles are easier to escape from restrain after collision, high concentration regions can also be found near the walls of the bed.

Effect of interstitial fluid on the distribution of granular temperature

Granular temperature is defined as the mean value of square of particle velocity fluctuations at three directions. It is defined as follows for a two dimensional fluidization system.

$$\theta = \frac{1}{3}(2\theta_x + \theta_y) = \frac{1}{3}(2\langle v_x^2 \rangle + \langle v_y^2 \rangle) \qquad (30)$$

Where θ_x、θ_y are the radial and axial particle velocity fluctuation squared, respectively.

Figure 6 shows the relationship between granular temperature and solid fraction for dry and wet particles at different superficial velocities. Similar to that for liquid-solid fluidization system, granular temperature increase with the solid fraction at low particle concentration to its maximum value and then decreases at higher solid fraction. Granular temperature is higher when increasing the superficial velocity of gas phase. When the effect of liquid film is considered, granular temperature differs a lot at low superficial velocities where liquid bridge effect plays an important role.

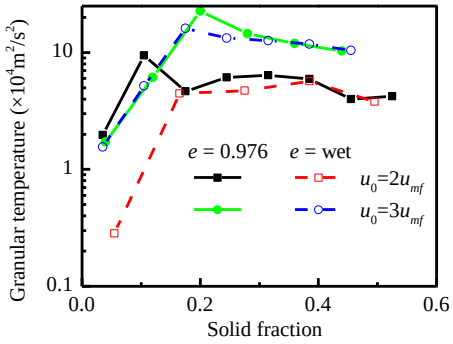

Figure 6: Granular temperature distribution as a function of solid fraction

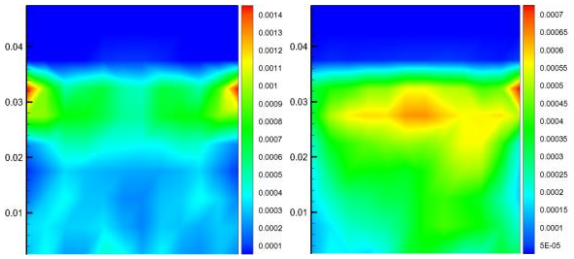

(a) θ_x contours

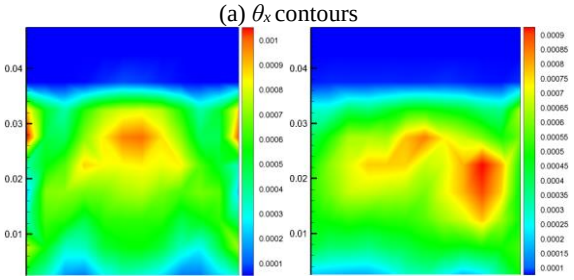

(b) θ_y counters

Figure 7: θ_x and θ_y counter distribution for dry (left) and wet (right) particles at superficial velocity $u_0 = 2u_{mf}$

Figure 7 shows the horizontal and vertical granular temperature distributions for dry and wet particles at superficial velocity $u_0 = 2u_{mf}$. Radial and axial fluctuations of dry particles are stronger than those of wet particles. Under the same condition, particle velocity fluctuations at axial direction are more intense than fluctuations at radial direction. From Figure 7 (b), axial velocity fluctuations reach the peak at the centre of the bed, and this area is concurrent with the bubble. It can be observed that granular temperature is anisotropic, and the axial velocity

fluctuation plays the dominant role since the flow direction is concurrent with the axial direction.

Figure 8 shows the counters of θ_y/θ_x. One can find that for a fixed bed height, differences between central and near-wall fluctuations are more prominent for the dry particles than those for the wet particles, and θ_x/θ_y are more homogeneous for the wet particles.

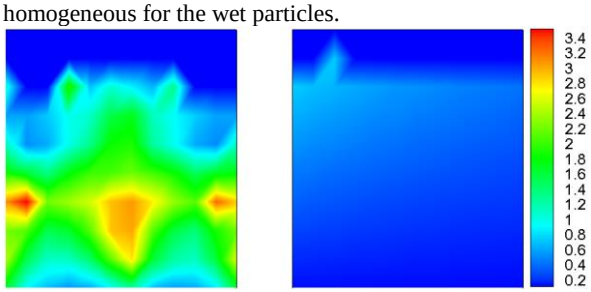

Figure 8: Distribution of θ_y/θ_x for dry (left) and wet (right) particles

CONCLUSION

The dynamic restitution coefficient model combined with DEM is employed to simulate the gas-solid fluidized bed of wet particles in this simulation. Simulated results show that the dynamic restitution coefficient model is capable of predicting the energy dissipation in the process of collision due to the presence of liquid film in the gas-solid fluidized bed. And the effect of interstitial fluid on the particle velocity, solid fraction and granular temperature is obtained.

Simulated results indicate that the axial and radial velocity distributions show obvious differences for dry particles, but the differences become weak for wet particles. For dry particles, the formation, rise and break of bubbles in the bed can be easily observed for dry particles, while wet particles are eager to aggregate due to the presence of liquid film. For dry particles, granular temperature behaves stronger anisotropic characteristics, especially at the centre and near-wall region, where differences between axial and radial fluctuations are obvious. Simulation results show that axial velocity fluctuations play the dominant role in the fluidization process, and velocity fluctuations turn to be weak for wet particles. Effects of 3D simulations will be conducted in the near future.

ACKNOWLEDGEMENT

This work was supported by the National Natural Science Foundation of China through grant no. 51106039, and Project 51121004, Natural Science Foundation of Heilongjiang Province through Grant No. E201205.

REFERENCES

HOLLAND D. J., MULLER C R, DENNIS J. S., et al. (2008), "Spatially Resolved Measurement of Anisotropic Granular Temperature in Gas-Fluidized Beds". *Powder Technology*, **182**, 171-181.

CUNDALL, P. A., STRACK, O. D. L., (1979), "A Discrete Numerical Model for Granular Assemblies". *Geotechnique*, **29**, 47-65.

DARABI P., POUGATCH K., SALCUDEAN M., et al. (2009), "A Novel Coalescence Model for Binary Collision of Identical Wet Particles". *Chemical Engineering Science*, **64**, 1868-1876.

WEN C. Y., YU Y. H. (1966), "Mechanics of Fluidization". *American Institute of Chemical Engineers Symposium Series*, **62**, 100-111.

GIDASPOW D., (1994), "Multiphase Flow and Fluidization : Continuum and Kinetic Theory Descriptions". New York, *Academic Press*.

JOSEPH G. G., HUNT M. L., (2004), "Oblique Particle-Wall Collisions in a Liquid", *J. Fluid Mech*, **510**, 71-93.

APOSTOLOU K., HRYMAK A. N., (2008), "Discrete Element Simulation of Liquid-Particle Flows", *Computers and Chemical Engineering*, **32**, 841-856.

GOLLWITZER F., REHVERG I., KRUELLE C. A., et al., (2012), "Coefficient of Restitution for Wet Particles", *Physical Review E*, **86**, 011303.

